Journal of Alloys and Compounds 509 (2011) 5683–5687

Contents lists available at ScienceDirect

Journal of Alloys and Compounds

journal homepage: www.elsevier.com/locate/jallcom

Growth and transport properties of oriented bismuth telluride films

Yuan Deng[a,*], Hui-min Liang[a], Yao Wang[a], Zhi-wei Zhang[a], Ming Tan[a], Jiao-lin Cui[b,*]

[a] Beijing Key Laboratory of Special Functional Materials and Film, School of Chemistry and Environment, Beihang University, Beijing 100191, China
[b] Materials Engineering Institute, Ningbo University of Technology, Ningbo 315016, China

ARTICLE INFO

Article history:
Received 8 December 2010
Received in revised form 20 February 2011
Accepted 22 February 2011
Available online 1 March 2011

Keywords:
Thermoelectric materials
Thin films
Crystal growth
Nanostructured materials

ABSTRACT

Oriented n-type bismuth telluride thin films with various layered nanostructures have been fabricated by radio-frequency (RF) magnetron sputtering. The crystal structures and microstructures of the films were characterized by X-ray diffraction (XRD) and scanning electron microscopy (SEM), respectively. The transport properties including carrier concentration, mobility, Seebeck coefficient and in-plane electrical conductivity were measured, which showed strong microstructure-dependent behaviors. The relationship between morphologies and transport properties of the films was explored. The optimal morphology and transport properties of films were obtained at the substrate temperature of 350 °C under the pressure of 1.0 Pa with oriented layered structure. Based on these results, a formation mechanism of these nanostructures is proposed and discussed. The interfaces and grain boundaries formed in these layered structures are beneficial to the reduction in thermal conductivity, which could result in potential TE films with high *ZT* value.

1. Introduction

Thermoelectric (TE) materials have attracted much attention due to their applications in power generators [1], coolers [2,3] and novel type sensors [4]. The thermoelectric figure of merit *ZT*, is defined as $ZT = \sigma S^2 T/\kappa$, where S, σ, κ, T are Seebeck coefficient, electrical conductivity, thermal conductivity, and absolute temperature, respectively. The *ZT* value can be significantly improved in low-dimensional materials owing to the effect of quantum confinement of charge carriers and phonon scattering at the boundaries and interfaces [5,6]. Several materials with special nanostructures, such as nanoplates, film, nanotubes and nanowires, have been synthesized in recently years, which show promising thermoelectric properties [7–11]. The greatly improved *ZT* value to 2.4 was first reported in Bi_2Te_3/Sb_2Te_3 superlattice thin film by Venkatasubramanian et al. [10]. Another high *ZT* value of 2.65 was obtained in Bi_2Te_3 film fabricated by pulsed laser deposition (PLD) [11].

Thin films with layered nanostructure are beneficial for the transport of carriers along the in-plane direction owing to the restriction of the periodic interfaces, and the carrier density along the in-plane direction can be enhanced to give a higher σ. On the other hand, the thermal conductivity can be significantly reduced due to the phonon scattering at the interfaces. Moreover, as Micro-Electro-Mechanical Systems (MEMS) develops rapidly, thin films have attracted an extensive interest because they can solve the integration problems of micro devices fabrication at the chip level [12,13]. Thus, many works have been focus on the fabrication of thin films. Bassi et al. prepared n-type Bi–Te thin film with a randomly layered nanostructure by pulsed laser deposition [14], which shows better thermoelectric performance than those of thin films without such layered nanostructure. Zhou et al. fabricated the Bi_2Te_3-based films with different morphologies by electrochemical deposition [15]. Duan et al. found the annealing plays a key role in the microstructural and transport properties of $Bi_2Te_{2.7}Se_{0.3}$ thin films under a flash evaporation process [16]. More recently, Bi_2Te_3 films with quintuple layers were formed by a mechanical exfoliation method [17–19], which show significant reduction in thermal conductivity. Magnetron sputtering has been widely adopted for large-scale fabrication of thin films with high quality. Liao et al. studied the deposition of Bi–Sb–Te thin films with average grain sizes of 26–83 nm [20]. Rhombohedral Bi_2Te_3 or hexagonal BiTe films were deposited by the variation of substrate temperature, which show the maximum power factor of 3 $\mu W/cm\,K^2$ at 225 °C [21]. These films are generally random stacks of grains on the substrate without any ordered nanostructure. It is still challenging to prepare thin film with oriented crystal growth on the substrate. In this paper, we prepared oriented bismuth telluride thin films with various layered nanostructures in large-scale using a simple RF magnetron sputtering method. The substrate temperature and working pressure play key roles in controlling of the morphologies of the films. The relationship between structures and transport properties has been discussed and the formation mechanism of these films is proposed.

* Corresponding authors. Fax: +86 10 82313482.
E-mail addresses: dengyuan@buaa.edu.cn (Y. Deng), cuijl@nbip.net (J.-l. Cui).

0925-8388/$ – see front matter © 2011 Elsevier B.V. All rights reserved.
doi:10.1016/j.jallcom.2011.02.123

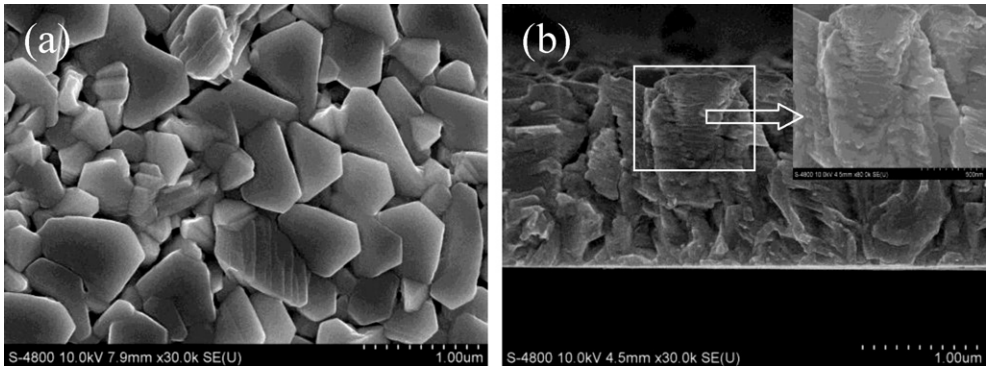

Fig. 1. SEM images of oriented layered Bi_2Te_3 film (a) surface image, (b) cross-sectional image, an inset shows the enlarged image of selected area in (b).

2. Experimental details

Thin films were deposited by RF magnetron sputtering on quartz glass wafer at temperature range from 200 to 400 °C. Before deposition, substrates were cleaned thoroughly successively by acetone, alcohol and deionized water for 15 min in ultrasonic bath. Commercial hot-pressed Bi_2Te_3 target (99.99%) was used and the distance between target and substrate was maintained at 60 mm. The working pressure was set from 0.7 to 1.0 Pa. All the films in this work were prepared with sputtering power 50 W.

XRD patterns were taken from a Rigaku D/MAX 2200 PC automatic X-ray diffractometer with Cu Kα radiation. The surface cross-sectional morphologies and composition of the films were analyzed by field emission scanning electron microscopy (FE-SEM) and energy dispersive spectrometer (EDS) (HITACHIH, S-4800). The Hall coefficient was measured using a four-probe method with Hall

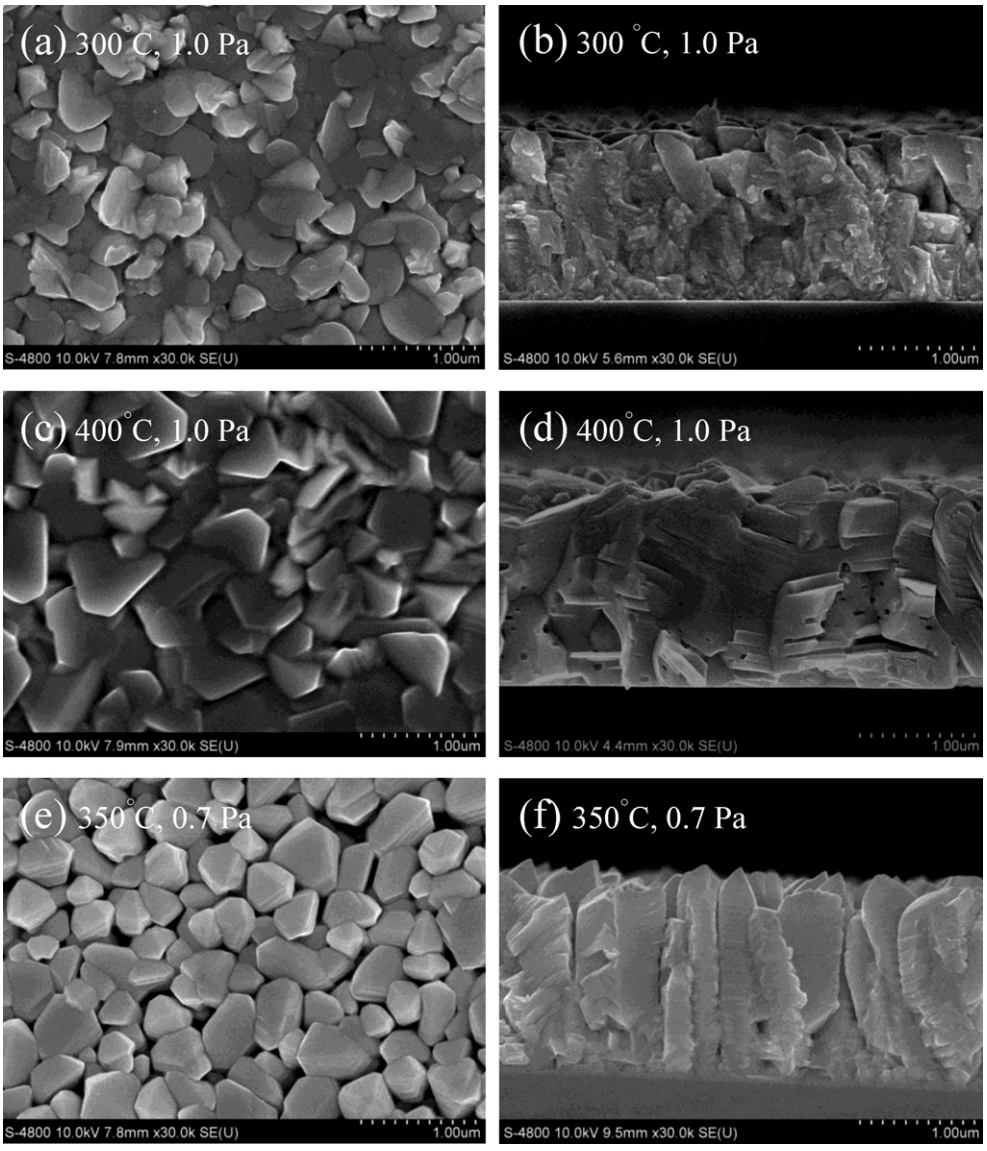

Fig. 2. Surface and cross-section images of the films deposited at different deposition conditions: (a, b) (300 °C, 1.0 Pa); (c, d) (400 °C, 1.0 Pa), (e, f) (350 °C, 0.7 Pa).

effects measurement (ECOPIA HMS-3000) at the room temperature. The in-plane electrical conductivity (σ) and Seebeck coefficient (S) were measured over a temperature range of 300–450 K by ZEM-3 (Ulvac Riko Inc.) with a self-made test holder for film measurement.

3. Results and discussion

Layered-grown oriented bismuth telluride thin film was successfully prepared on quartz glass substrate with substrate temperature 350 °C and working pressure 1.0 Pa. As shown in Fig. 1, the film is composed of grains in hexagonal shape with the grain size 0.7–0.8 μm. The inset in Fig. 1b shows the detail cross-sectional morphology of the film: stacking by uniform hexagonal layers with ~50 nm in thickness. XRD pattern of the film is shown in Fig. 3a, demonstrating a well-crystallized Bi_2Te_3 film. All the peaks could be matched to the indexes of rhombohedral phase $R\bar{3}m$ (JCPDS 15-0863). It can be seen clearly that the peaks (0 0 6) and (0 0 15) are stronger than those specified in the standard PDF card, indicating a preferred growth along *c*-axis orientation, which could also been observed from the SEM images.

During deposition process, it was found that the substrate temperature and working pressure play important roles in the formation of different morphologies of the films. Films with different layered nanostructures, like nanoparticles, compactly layered structures, columnar structures, have also been observed under different deposition conditions.

When the substrate temperature decreases from 350 to 300 °C, the film is the stack of particles with size of 200 nm without preferred crystal orientation (Fig. 2a and b). All the XRD peaks of the film (Fig. 3b) exhibit much weaker intensity than those of 350 °C, presenting a low crystalline quality. It is obvious that decreasing the temperature is not beneficial for the diffusion of the atoms in the substrate, but more particles than layered crystals form in the film. When the substrate temperature increases from 350 °C to 400 °C, the grains in the layered film grow thicker and larger, and some grains sinter together due to higher temperature (shown in Fig. 2c and d). It is very interesting that the Bi_2Te_3 film does not peel off the substrate even at the temperature as high as 400 °C, revealing

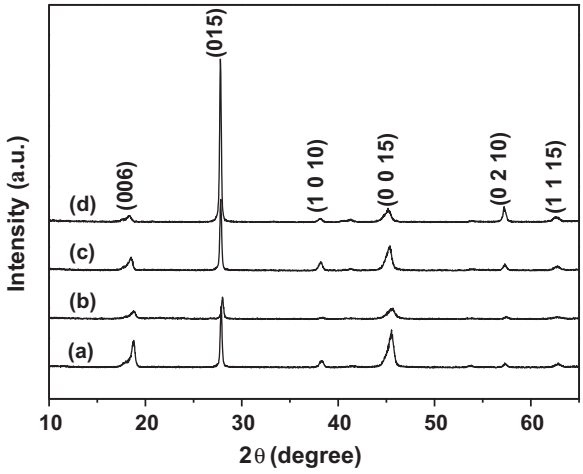

Fig. 3. XRD patterns of the films fabricated at different conditions: (a) 350 °C, 1.0 Pa; (b) 300 °C, 1.0 Pa; (c) 400 °C, 1.0 Pa; (d) 350 °C, 0.7 Pa.

well adhesion strength between the film and the substrate under high temperature. The intensities of (0 0 6) and (0 0 15) peaks of the films deposited at 400 °C become weaker than those at 350 °C (shown in Fig. 3c). These results indicate that the thin films fabricated at 350 °C have a preferred crystal orientation along the *c*-axis direction. This is consistent with the results of SEM images.

The deposition temperature was then fixed at 350 °C, and the working pressure was decreased to 0.7 Pa. As shown in Fig. 2e, the grain size of the film is uniformly distributed of about 200 nm, which is much smaller than the film grown under 1 Pa. From the cross-sectional image (Fig. 2h), the film is grown in columnar grain from the bottom to top, and each column is composed of layered structure with each layer ~120 nm in thickness. In this case, the nucleation in the vertical direction is faster than the crystal growth in plane. Then island growth mode dominates under the condition of 350 °C and 0.7 Pa, so the columnar grains form. From XRD patterns shown in Fig. 2d, peak (0 1 5) is ultra-strong indicating a

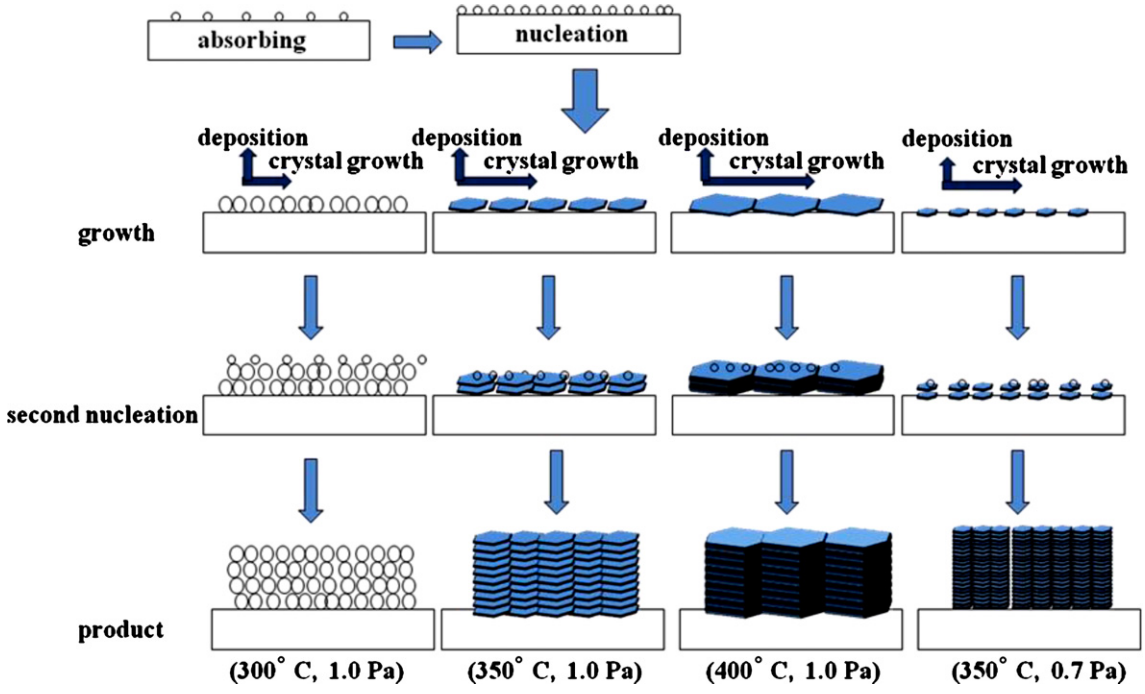

Fig. 4. Growth mechanisms of oriented Bi_2Te_3 films with different microstructures.

preferred growth along (0 1 5) direction, which is different from the preferred growth along (0 0 *l*) direction when pressure increases to 1.0 Pa.

The thickness of all above films deposited for the same period of time is approximately 1.5 μm, which means the deposition rate of Bi_2Te_3 atoms is much higher than the crystal growth of nuclei. Thus substrate temperature and working pressure affect both the nucleation process and the crystal growth, and the thickness of the films is closely related to the deposition time. Although the detailed growth mechanism of oriented Bi_2Te_3 film is still not clear, the above results allow us to suggest a possible process to obtain Bi_2Te_3 film with special structures. The growth process of the films is illustrated in Fig. 4, which is based on an island growth mode with different crystal growth rate.

Firstly, Bi and Te atoms were sputtered and deposited on the surface of substrate. Then, nucleation began and hexagonal islands formed due to the anisotropic diffusion. Usually, for Bi_2Te_3 material, the preferential growth of (0 1 5) crystal plane is easy to form hexagonal flakes, while the preferential growth of (0 0 *l*) and (0 1 5) crystal planes result in the formation of rods with oriented layer rather than that of hexagonal flakes. Thus the key for fabricating Bi_2Te_3 film with oriented layered nanostructure is to keep a proper crystal growth rate. When the substrate temperature is above 350 °C, the crystal growth rate of Bi_2Te_3 atoms was higher than deposition rate, so the nuclei had enough time to grow into hexagonal flakes before a new nucleation occurred. When the crystal growth rate of Bi_2Te_3 atoms was lower than deposition rate (e.g., substrate temperature below 350 °C and work pressure below 1 Pa), the nuclei can only grow to small flakes or particles. Next, a new nucleation and growth process happened on the already formed film, to form oriented grown multilayer. The potential energy at the edge of the islands is much higher than that at the center, so ad-atoms deposited on the islands were incorporated within the island itself. The elastic strain energy on the top parts of islands is usually much lower than that at the bottom. As a result, the surface diffusion due to the strong uneven distribution of strain energy, drives ad-atoms to climb up to the tops of islands, and gives rise to the rapid radial growth of 3D islands. The adjacent islands blocked ad-atoms come from planar direction, and caught hold of ad-atoms deposited from the radial directions. Then the interspaces among islands form and led to the growth of columnar grains perpendicular to the glass substrate. Finally, oriented films with different structures were obtained on the substrate.

The transport properties of these TE films with different microstructures as a function of temperature were measured and shown in Fig. 5. Seebeck coefficients (*S*) of all the films exhibit negative values, indicating an n-type semiconductor (shown in Fig. 5a), and the magnitude of Seebeck coefficients of all the films increase as temperature increases. Generally, film with oriented layered structure has the largest absolute *S* value, i.e., −85 μV/K at 450 K, and film in columnar structure shows the smallest one. Seebeck coefficient of the films composed of nanoparticles and thicker layers have almost identical values, i.e., from about −60 μV/K at 300 K increase to −74 μV/K at 450 K.

The electrical conductivities decrease with the increase of measuring temperature (see Fig. 5b), indicating a metallic like behavior [22]. We can see that the film with layered structures has maximum electrical conductivity of 1.8×10^5 S/m at room temperature, while the film composed of nanoparticles and thicker layers have electrical conductivities of about 1.4×10^5 S/m and 2.2×10^5 S/m, respectively. When the film microstructure turns to be columnar structure, the conductivity increases to 3×10^5 S/m, which is 2–3 times larger than those of state-of-the-art bulk alloys [23].

Power factor *p*, $p = \sigma S^2$, was calculated as shown in Fig. 5c. With the increase of temperature, power factors of all the films increase.

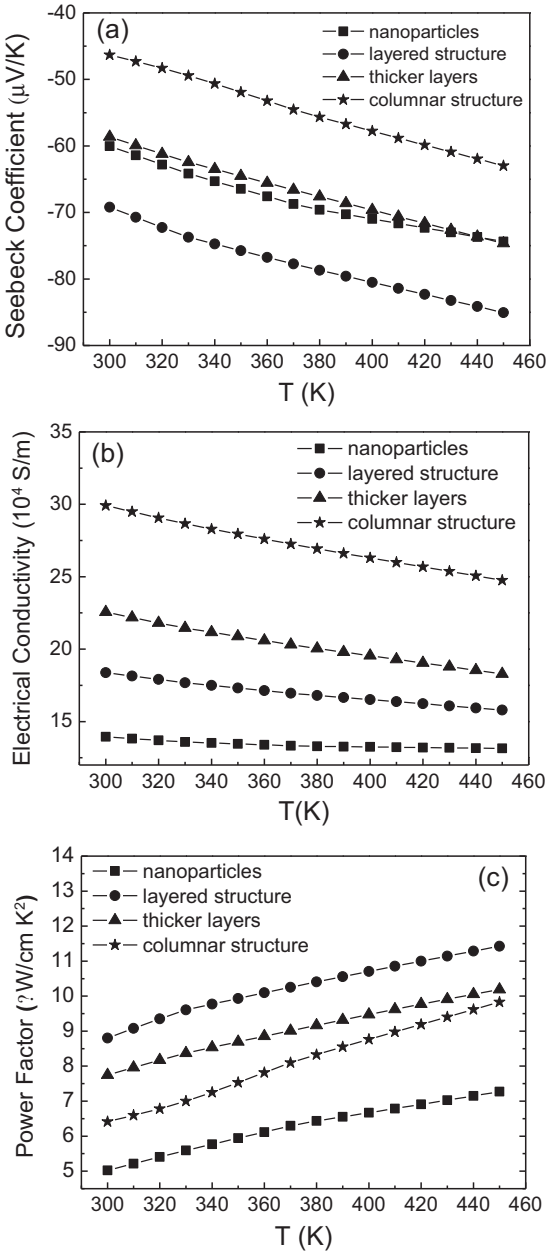

Fig. 5. Transport properties of different morphologies of Bi_2Te_3 films.

The film with oriented layered structure shows the highest power factor increasing from 8.8 to 11.4 μW/cm K^2 due to its special microstructure. The film with thicker layered structure exhibits the second large power factor value, the film with columnar structure the third, and the film with nanoparticles the lowest. It is observed that the films with more connected and compact structures possess higher power factor. Compared to previous reports on bismuth telluride films prepared by sputtering, e.g., 4×10^{-4} W/m K^2 reported by Huang et al. [24] and 9×10^{-4} W/m K^2 reported by Kim et al. [25], our films with controlled microstructure show an improved power factor. However, if compared to the films deposited by PLD [16] and MOCVD [26], the Seebeck coefficients of our films are still low and need to be further increased to enhance the power factor.

To elucidate the origin of the improved transport properties of the TE film, especially of the much higher conductivity compared with previous studies on Bi_2Te_3 films which have similar Seebeck

Table 1
Transport properties and compositions of thin films deposited at different conditions measured at room temperature.

Deposition conditions		Morphologies	Carrier concentration (10^{21}/cm^3)	Carrier mobility (cm^2/V s)	Electrical conductivity (10^4 S/m)	Seebeck coefficient (μV/K)	Power factor (μW/cm K^2)	Bi/Te atomic ratio
300 °C	1.0 Pa	Nanoparticles	−1.05	8.3	13.9	−60	5.0	43.1/56.9
350 °C	1.0 Pa	Layered structure	−0.95	12.1	18.4	−70	8.8	43.4/56.6
400 °C	1.0 Pa	Thicker layers	−1.31	10.7	22.6	−58	7.7	48.2/51.8
350 °C	1.0 Pa	Columnar structure	−2.46	7.5	29.9	−46	6.4	42.8/57.2

coefficient values, Hall effects measurement was carried out at room temperature to study the concentration and mobility of the carriers. And meanwhile, the composition analyses by EDS were also considered. The carriers, transport properties and the atomic ratio of Bi and Te elements in Bi_2Te_3 films in various microstructures are summarized in Table 1. The film with compact layered structures has the higher mobility (12.1 cm^2/V s) than that with thick layer (10.7 cm^2/V s). Due to the fact that grain boundaries act as barriers to the carriers, the particle and columnar structured films with higher grain boundaries showed reduced carrier mobility.

On the other hand, the compositions of the films affect the carrier concentrations. As shown in Table 1, all the films prepared under our experimental conditions show Te deficiency to the extent of different levels. For the films grown under the same pressure, the higher the temperature, the more the Te lost, thus enhancing concentration of n-type carriers. However, for the film grown under lower pressure with columnar structure, the atomic ratio of Bi/Te shows the smallest deviation from the stoichiometric ratio, but possesses the highest value of carrier concentration 2.46×10^{21}/cm^3, which results in its high electrical conductivity but in decreased Seebeck coefficient accordingly. The high carrier concentration not only comes from the contribution of the Te deficiency, but also probably from the large numbers of defects which trap the holes and produce more electrons.

4. Conclusions

In summary, n-type bismuth telluride thin films with various layered nanostructures were fabricated by RF magnetron sputtering. The crystal growth rate plays an important role in the controlling the morphologies of the films. Thin films with oriented layered structure, nanoparticles, thicker layers and columnar structure were successfully prepared due to the competition between the crystal growth in the planar direction and the nucleation in radial direction. The films with such special structure also exhibit attractive thermoelectric properties. Optimal TE properties were obtained in the film with oriented layered structure with Seebeck coefficient $S \sim -70$ μV/K at room temperature, −85 μV/K at 450 K, and power factor 8.8 μW/cm K^2 at room temperature, 11.4 μW/cm K^2 at 450 K, respectively.

Acknowledgements

The work was supported by National Natural Science Foundation of China under Grant Nos. 50772005, 51002006, the National High Technology Research and Development Program of China under Grant No. 2009AA03Z322 and Beijing Technology Topic Program under Grant No. Z08000303220808.

References

[1] L.D. Chen, X.Y. Li, W. Jiang, D.G. Zhao, L. He, J. Alloys Compd. 477 (2009) 425–431.
[2] M. Takashiri, S. Tanaka, M. Takiishi, M. Kihara, K. Miyazaki, H. Tsukamoto, J. Alloys Compd. 462 (2008) 351–355.
[3] B.C. Sales, Science 295 (2002) 1248–1249.
[4] M. Fardy, A.I. Hochbaum, J. Goldberger, M.M. Zhang, P.D. Yang, Adv. Mater. 19 (2007) 3047–3051.
[5] L.D. Hicks, T.C. Harman, X. Sun, M.S. Dresselhaus, Phys. Rev. B 53 (1996) 10493–10496.
[6] W.J. Xie, X.F. Tang, Y.G. Yan, Q.J. Zhang, T.M. Tritt, J. Appl. Phys. 105 (2009) 113713.
[7] Z. Wang, F.Q. Wang, H. Chen, L. Zhu, H.J. Yu, X.Y. Jian, J. Alloys Compd. 492 (2010) 50–53.
[8] Q. Zhao, Y.G. Wang, J. Alloys Compd. 497 (2010) 57–61.
[9] L.N. Zhou, X.B. Zhang, X.B. Zhao, C.X. Sun, Q. Niu, J. Alloys Compd. 502 (2010) 329–332.
[10] R. Venkatasubramanian, E. Siivola, T. Colpitts, B. O'Quinn, Nature 413 (2001) 597–602.
[11] J. Walachová, R. Zeipl, J. Zelinka, V. Malina, Appl. Phys. Lett. 87 (2005) 081902.
[12] G.J. Snyder, J.R. Lim, C.K. Huang, J.P. Fleurial, Nat. Mater. 2 (2003) 528–531.
[13] G.E. Bulman, E. Siivola, B. Shen, R. Venkatasubramanian, Appl. Phys. Lett. 89 (2006) 122117.
[14] A. Li Bassi, A. Bailini, C.S. Casari, F. Donati, A. Mantegazza, M. Passoni, V. Russo, C.E. Bottani, J. Appl. Phys. 105 (2009) 124307.
[15] L.Q. Qiu, J. Zhou, X. Cheng, R. Ahuja, J. Phys. Chem. Solids 71 (2010) 1131–1136.
[16] X.K. Duan, Y.Z. Jiang, Appl. Surf. Sci. 256 (2010) 7365–7370.
[17] D. Teweldebrhan, V. Goyal, M. Rahman, A.A. Balandin, Appl. Phys. Lett. 96 (2010) 053107.
[18] D. Teweldebrhan, V. Goyal, A.A. Balandin, Nano Lett. 10 (2010) 1209.
[19] V. Goyal, D. Teweldebrhan, A.A. Balandin, Appl. Phys. Lett. 97 (2010) 133117.
[20] C.N. Liao, Y.C. Wang, H.S. Chu, J. Appl. Phys. 104 (2008) 104312.
[21] D.H. Kim, E. Byon, G.H. Lee, S. Cho, Thin Solid Films 510 (2006) 148–153.
[22] F.R. Yu, J.J. Zhang, D.L. Yu, J.L. He, Z.Y. Liu, B. Xu, Y.J. Tian, J. Appl. Phys. 105 (2009) 094303.
[23] D.H. Kim, T. Mitani, J. Alloys Compd. 399 (2005) 14–19.
[24] H. Huang, W. Luan, S. Tu, Thin Solid Films 517 (2009) 3731–3734.
[25] D.H. Kim, G. Lee, Mater. Sci. Eng. B 131 (2006) 106–110.
[26] Y.C. Jung, J.H. Kim, S.H. Suh, B.K. Ju, J.S. Kim, J. Cryst. Growth 290 (2006) 441–445.